Acta Crystallographica Section F
Structural Biology and Crystallization Communications
ISSN 1744-3091

Atomic resolution structure of the double mutant (K53,56M) of bovine pancreatic phospholipase A_2

K. Sekar,[a,b]* M. Yogavel,[c] D. Gayathri,[c] D. Velmurugan,[c] R. Krishna,[a] M.-J. Poi,[d] Z. Dauter,[e] M. Dauter[e] and M.-D. Tsai[d,f]

[a]Bioinformatics Centre, Indian Institute of Science, Bangalore 560 012, India, [b]Supercomputer Education and Research Centre, Indian Institute of Science, Bangalore 560 012, India, [c]Department of Crystallography and Biophysics, University of Madras, Guindy Campus, Chennai 600 025, India, [d]Departments of Chemistry and Biochemistry and the Ohio State Biochemistry Program, The Ohio State University, Columbus, OH 43210, USA, [e]Synchrotron Radiation Research Section, National Cancer Institute, Brookhaven National Laboratory Building, Upton, NY 11973, USA, and [f]Academia Sinica, Taiwan

Correspondence e-mail: sekar@physics.iisc.ernet.in, sekar@serc.iisc.ernet.in

Received 24 October 2005
Accepted 7 December 2005
Online 16 December 2005

PDB Reference: K53,56M bovine pancreatic PLA_2, 2bax.

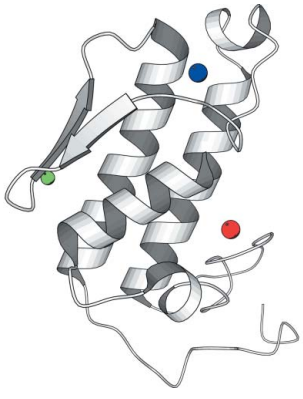

The structure of the double mutant K53,56M has previously been refined at 1.9 Å resolution using room-temperature data. The present paper reports the crystal structure of the same mutant K53,56M refined against 1.1 Å data collected using synchrotron radiation. A total of 116 main-chain atoms from 29 residues and 44 side chains are modelled in alternate conformations. Most of the interfacial binding residues are found to be disordered and alternate conformations could be recognized. The second calcium ion-binding site residue Glu92 adopts two alternate conformations. The minor and major conformations of Glu92 correspond to the second calcium ion bound and unbound states.

1. Introduction

Phospholipases A_2 (PLA_2s) are widely distributed in nature and constitute a superfamily of enzymes that participate in a number of processes such as lipid metabolism, signal transduction and eicosanoid production (Dennis, 1997). PLA_2 enzymes are characterized into two (structurally and biochemically) distinct classes, namely cytosolic and secretory. The cytosolic PLA_2s (80–110 kDa) are present in many cell types and are involved in phospholipid metabolism and transmembrane signalling. The secretory PLA_2s (13–14 kDa) are abundant in mammalian pancreas and in reptile and insect venoms. PLA_2s specifically catalyze the hydrolysis of the ester linkage at the *sn*-2 position of the important membrane constituents glycerophospholipids (van Deenen & de Haas, 1963; Dennis, 1983), yielding free fatty acids and lysophospholipids, and thereby initiate the biosynthesis of inflammatory and allergic mediators, eicosanoids and platelet-activating factor (Scott & Sigler, 1994; Dennis, 1994).

PLA_2s display enhanced activity towards lipids in lamellar and micellar aggregates both in membranes and at other lipid–water interfaces (Ramirez & Jain, 1991; Jain *et al.*, 1995). An intriguing feature of PLA_2 is its 'interfacial activation', *i.e.* a substantial increase in enzymatic activity upon transition of the substrate from a monomeric to an aggregated state (Verger, 1976; Pieterson *et al.*, 1974). X-ray studies on PLA_2s (Fig. 1) have revealed similar tertiary structures of these enzymes with and without bound inhibitor. However, small structural differences were found in the structures solved using X-ray crystallography between the free and complexed forms of PLA_2 (Scott *et al.*, 1991). Recent crystallographic studies carried out in our laboratory on various triple mutants of recombinant bovine pancreatic PLA_2 (Rajakannan *et al.*, 2002; Sekar *et al.*, 2005) underscore the presence of a second calcium ion. Biochemical and enzyme-kinetics studies of the four cationic residues involving lysine (53, 56, 120 and 121) to methionine mutations show an incremental role in both substrate binding at the active site and enzyme binding at the lipid–water organized interface. To gain further understanding of the mutated residues, our laboratory has been working on the crystal structure analysis of individual and combined mutations of the four cationic residues. Here, we report the crystal structure of the double mutant K53,56M determined at atomic resolution.

Table 1
Crystal, relevant refinement and geometrical parameters of the atomic resolution model of the double mutant K53,56M.

Values in parentheses correspond to the highest resolution shell.

PDB code	2bax
Wavelength (Å)	0.979
Temperature (K)	100
Unit-cell parameters (Å, °)	$a = b = 46.057$, $c = 101.138$, $\alpha = \beta = 90$, $\gamma = 120$
V_M (Å^3 Da^{-1})	2.2
Z	6
Space group	$P3_121$
Resolution range (Å)	20.0–1.10 (1.14–1.10)
Unique reflections	50297 (4992)
Completeness of data (%)	98.3 (99.0)
R_{merge}	0.044 (0.216)
$I/\sigma(I)$	20.65 (9.66)
Protein atoms	955 (304 partial occupancies)
Calcium ions	1
Chloride ions	1
MPD atoms	112
Water sites	236
No. of parameters in the final run of *SHELXL*	14408
R_{work} for $F > 4\sigma$ (%)	11.45
R_{free} (%)	14.48
R_{work} for all data (%)	11.93
Ramachandran plot, residues in	
Most favoured regions (%)	88.2
Additionally allowed regions (%)	11.8
R.m.s. deviations	
Bond distances (Å)	0.013
Bond-angle distances (Å)	0.034
Luzzati coordinate error (Å)	0.015
Mean B factor (Å^2)	
All protein atoms	19.83
Main-chain atoms	17.37
Side-chain atoms	22.16

2. Materials and methods

2.1. Crystallization

Crystals were grown by the hanging-drop vapour-diffusion method at room temperature using the conditions described previously (Noel *et al.*, 1991; Yu *et al.*, 2000). In brief, the double-mutant protein was dissolved in 50 m*M* Tris buffer pH 7.2 containing 5 m*M* $CaCl_2$ to a final protein concentration of 17–20 mg ml^{-1}. The crystallization droplet contained 5 µl protein solution and 2 µl 60% MPD and the reservoir contained 1000 µl 70% MPD. Trigonal crystals appeared approximately after one week and grew to a final size of 0.40 × 0.40 × 0.50 mm.

2.2. Data collection and processing

To prepare for data collection (synchrotron radiation) at cryo-temperature, 15% glycerol was added to the mother liquor and the crystal was mounted and flash-frozen. X-ray data were collected to 1.1 Å on an ADSC Quantum 4 CCD detector at the X9B beamline of the National Synchrotron Light Source, Brookhaven National Laboratory, Upton, New York, USA. The X-ray wavelength was 0.979 Å. The diffraction images were processed with the *HKL*2000 suite (Otwinowski & Minor, 1997). A summary of the data-processing statistics is given in Table 1.

2.3. Structure solution and refinement

The structure was solved by molecular-replacement calculations using the atomic coordinates of the same double mutant reported previously (PDB code 1c74; Yu *et al.*, 2000). It was refined in a first step with isotropic B factors using the maximum-likelihood method with *REFMAC* (Murshudov *et al.*, 1997), which led to an R_{work} of 24.5% in a few cycles. Further refinement was performed in *SHELXL*97 (Sheldrick, 1997; Sheldrick & Schneider, 1997), starting from the fractional coordinates taken from the *REFMAC* model. A total of 2510 reflections (5%) were randomly selected from the full resolution range 20.0–1.1 Å for the calculation of R_{free} (Brünger, 1992). Firstly, 20 cycles of rigid-body refinement were carried out (resolution range of 20–2.5 Å) and the refinement converged to R_{work} = 34.2% (R_{free} = 36.4%). Secondly, conjugate-gradient least-squares isotropic refinement was carried out (resolution range 20.0–1.5 Å) and the refinement converged to R_{work} = 28.5% (R_{free} = 32.0%). The high initial values of the R factors primarily reflect the contribution and importance of the solvent atoms, despite the fact that a bulk-solvent correction according to the Babinet principle (Moews & Kretsinger, 1975) was used. When the best 74 water molecules and one Ca^{2+} were added, R_{work} fell to 22.8% (R_{free} = 25.1%). In the third step, the resolution range was extended to 1.1 Å. The electron-density maps were becoming progressively clearer, allowing unambiguous manual identification of further components in the solvent area, including 119 water molecules and one chloride ion as well as two MPD molecules. The chloride ion and the MPD molecules were not present in the room-temperature data published previously (Yu *et al.*, 2000). The isotropic refinement caused the R_{work} and R_{free} values to converge to 20.6 and 23.0%, respectively. Inspection of the difference electron-density maps revealed numerous patches of positive density near the main-chain atoms and well defined side-chain atoms. They were particularly prominent at the Trp3, Ser74, Ser78 and Glu92 side-chain atoms. Introduction of anisotropic displacement parameters in the next stage was accom-

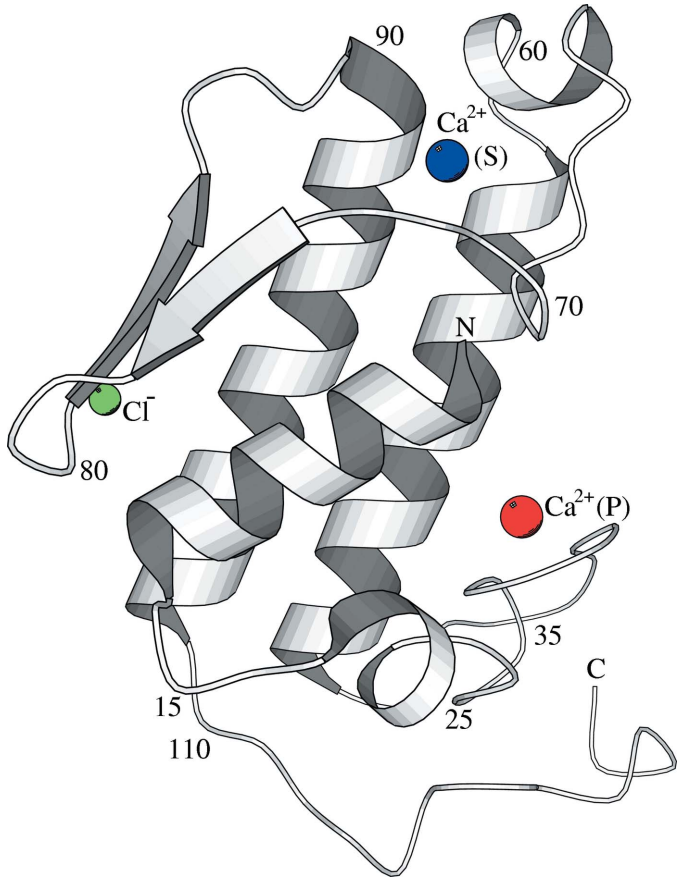

Figure 1
Ribbon diagram of the structure of recombinant bovine pancreatic PLA_2. N and C represent the N- and C-termini, respectively. The essential calcium ion (P), second calcium ion (S) and chloride ion (Cl^-) are also shown.

panied by a large fall (of about 6%) in both the R_{work} and R_{free} values. The anisotropic model was used for all atoms, including solvent atoms (the best and poorest, without distinction), and for alternative conformations of the residues, even with minor occupancies. According to the default settings of *SHELXL*97, the anisotropic displacement parameters were restrained (both DELU and SIMU) and the water O atoms were kept fairly isotropic (ISOR). The default geometrical restraints were used as implemented in *SHELXL*97, using the targets defined by Engh & Huber (1991) for refining the polypeptide geometry. In rounds 7–10, partially occupied water sites were added and adjusted manually. The criterion for adjusting occupancy was that no residual density should appear after *B*-factor refinement. The program *FRODO* (Jones, 1985) was deployed for model building and inspection of the electron-density maps. At stage 12, the refinement using default restraints converged to an R_{work} of 12.4% (R_{free} = 15.7%). The introduction of riding H atoms in the final round lowered the R_{work} by 1% and R_{free} by even more. The H atoms of the protein hydroxyl groups were also generated automatically, but their locations were verified manually for consistency with difference electron-density maps and plausible hydrogen-bonding interactions. In all cases, a satisfactory agreement was found. In the last round, all the test reflections were also included in the refinement of the final model and the final *R* factor converged to 11.5%. The refinement details are summarized in Table 1.

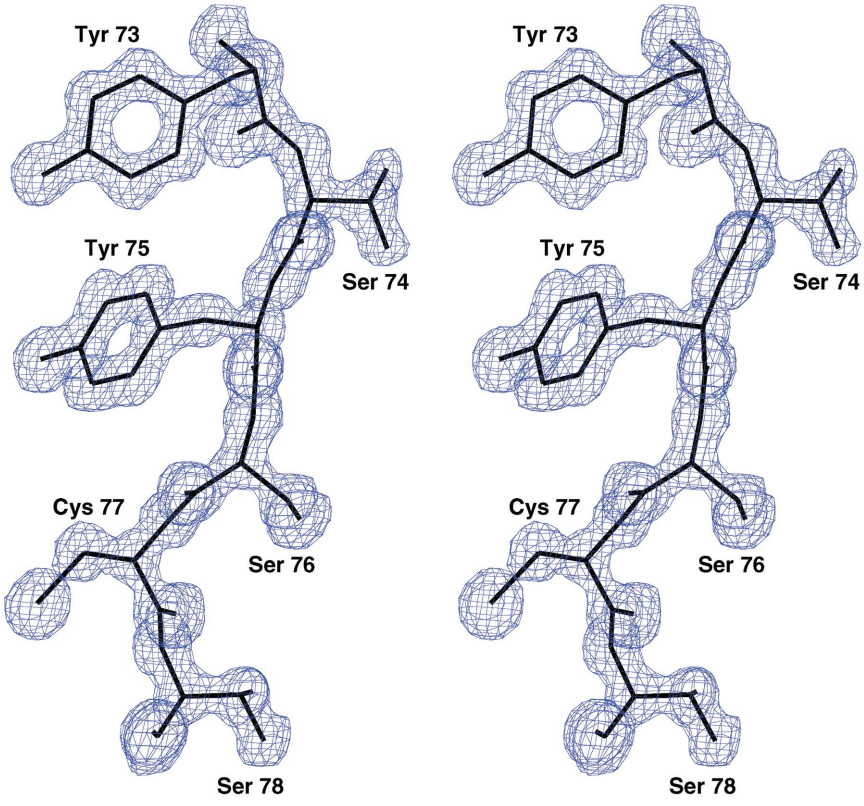

Figure 2
Stereoview of the difference electron density ($2|F_o| - |F_c|$) for the final refined model. The map was contoured at the 2σ level.

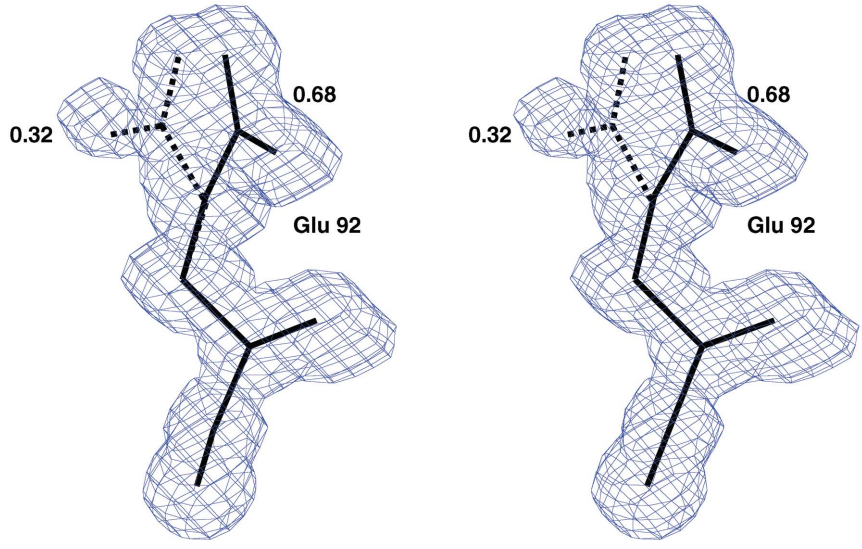

Figure 3
Stereoview of the two conformations of Glu92 and the difference electron-density map (1.2σ level). Dotted lines represent the minor conformation (occupancy = 0.32).

3. Results and discussion

3.1. Quality of the structure

The protein model is of very high quality and includes all atoms. In general, the electron density of the polypeptide chain is very clear and well ordered (except for residues 62–70 and 113–123). Even most disordered residues in alternate conformations are generally modelled without ambiguity. The complete main chain is visible (Fig. 2) in contiguous electron density ($2|F_o| - |F_c|$ map) above the 1.2σ level, including fragments that assume alternate/multiple conformations. A total of five MPD molecules and one chloride ion could be modelled in their respective density with confidence. More than 88% of the residues are in the most favoured regions of the Ramachandran plot (Ramachandran *et al.*, 1963) and no residues are observed in the disallowed region. 236 water sites were located. A total of 29 peptide bonds and 44 side chains are modelled in two discrete conformations. Three residues, Thr70, Asn71 and Lys113, have their side chains refined to occupancies lower than 1.0 (0.56, 0.70 and 0.63, respectively), but no alternate conformations could be recognized for these residues. Other stereochemical parameters of the refined model are discussed below.

3.2. Calcium-binding site

The catalytically important primary calcium ion in the active site is essential for both substrate binding and catalysis. The average coordination distance is 2.41 Å and this agrees well with the distance of 2.39 Å from the survey of the small-molecule database for a calcium ion with a coordination number of seven (Harding, 1999). The calcium ion is located at 2.46 and 2.52 Å from

the carboxylate O atoms of Asp49, thus giving rise to an asymmetry of 0.04 Å; the corresponding values for the wild-type structure (Steiner *et al.*, 2001) and the triple mutant (Sekar *et al.*, 2005) are 0.03 and 0.04 Å, respectively. The structures of the recently reported monoclinic forms of the bovine pancreatic PLA_2 triple mutants K56,120,121M (Rajakannan *et al.*, 2002) and K53,56,121M (Sekar *et al.*, 2005) detail the location of the secondary calcium ion-binding site involving the residues Asn71, Asn72 and Glu92. In the present structure there is no second calcium ion, because the side chain of the second calcium-binding residue Glu92 and the main-chain Asn72 adopt two conformations (Figs. 3 and 4). The double conformations of Glu92 corresponds to the second calcium bound and unbound free form of bovine pancreatic PLA_2.

3.3. Chloride ion

During the progress of the refinement, the most significant feature noticed in the difference electron-density map ($|F_o| - |F_c|$) is an additional positive density (above the 6σ level) at the modelled water molecule which is hydrogen bonded to the peptide amino group of Ile82, the side-chain N atom of Lys12 and a water molecule. The large peak suggests the presence of an ion near Arg100 and we interpreted this as a chloride ion (since $CaCl_2$ was used in the crystallization buffer). The position of the chloride ion was confirmed with the triple-mutant structure (S-SAS data; Sekar *et al.*, 2004), the atomic resolution structure of the triple mutant K53,56,121M (Sekar *et al.*, 2005) and the wild-type atomic resolution structure of PLA_2 (Steiner *et al.*, 2001). The refined chloride ion has an occupancy of 0.75. This position was occupied by a water molecule in the previously reported model of the same double mutant (Yu *et al.*, 2000). The position of the chloride ion is further confirmed by the wild-type atomic resolution structure of native PLA_2 (Steiner *et al.*, 2001). The chloride ion has four ligands; namely, the backbone N atom of Ile82, the side-chain N atom of Lys12, the major conformer of the side chain of Glu81 $O^{\varepsilon1}$ and a water molecule. This water molecule is further hydrogen bonded to the guanidium group of Arg100. The average coordination distance of the chloride ion is 2.96 Å.

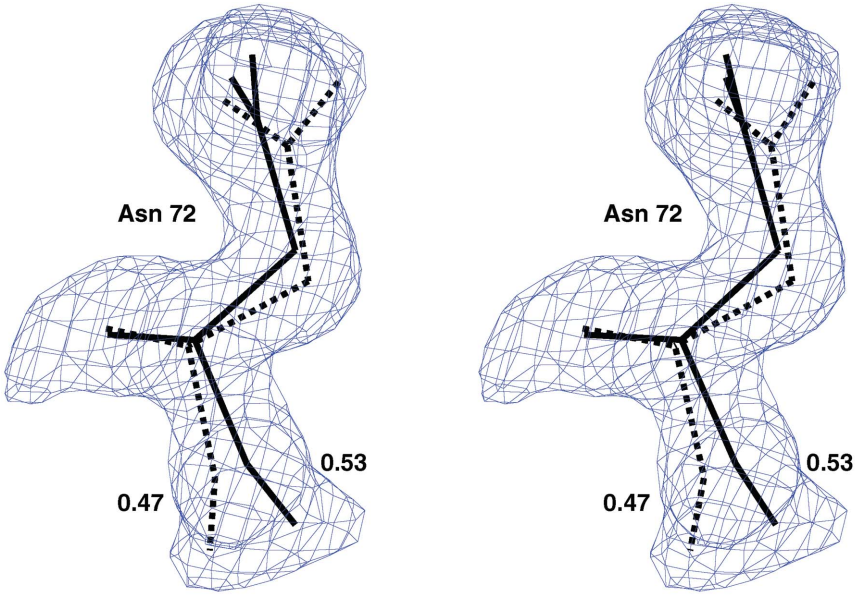

Figure 4
A stereoview of the alternate conformations of Asn72 along with the difference electron-density map (1.2σ level). The occupancy values are also shown. The minor conformation is shown by dotted lines.

3.4. Water structure

The refined model contains 236 water sites with an average B_{eq} value of 29.86 $Å^2$, of which 27 water sites are modelled in alternate positions with the sum of their occupancies fixed to 1.0 during refinement. Of the 236 water sites, 201 are in the first hydration shell, while 30 are in the second hydration shell. The remaining five water molecules do not have contacts and are treated as isolated water molecules. The first hydration shell water molecules are involved in 443 contacts (between 2.25 and 3.6 Å) with the polar atoms of the protein molecule (198 contacts are with the backbone polar atoms and 245 contacts with the side-chain polar atoms). A total of 74 water molecules are common to the present and the previously reported (Yu *et al.*, 2000) models.

3.5. Temperature factor and anisotropic displacement parameters

The pattern of atomic displacement parameters along the protein chain differs very greatly from that of the wild-type (Steiner *et al.*, 2001) and the triple mutant K53,56,121M (Sekar *et al.*, 2005) structures. The mean isotropic temperature factors of the protein and the solvent atoms are 20 and 30 $Å^2$, respectively. For the main-chain atoms, the plots are identical in the low-displacement areas, whereas higher anisotropy is observed at reduced temperature in the areas of increased mobility. This may be rationalized by the fact that lowering the temperature reduces the dynamic but not the static disorder. This confirms that increased mobility and resolved disorder have anisotropic character. A similar proportion of disordered residues is reported in the atomic resolution structures of wild-type and triple-mutant PLA_2. The average anisotropy factor of the protein atoms is 0.466 (131) and the corresponding values for the solvent atoms and the MPD atoms are 0.480 (135) and 0.417 (126), respectively.

3.6. Comparison of side-chain conformations

Few residues of the present model assume different conformations when compared with the previously reported model (Yu *et al.*, 2000). In particular, residue Glu87 adopts a different conformation and is bent towards the solvent region. The electron density of Glu87 in the present model is clear. In the previously reported model, the side-chain O atoms of Glu87 are hydrogen bonded to Ser74, where as in the present atomic resolution model the side-chain O atoms of Glu87 are hydrogen bonded to the water molecules. However, the electron density of the residue Trp3 was poor in the present model; it takes two conformations and electron density is reasonably clear. Trp3 is located at the active-site mouth and a partially occupied MPD molecule is also present at the surface of the active site.

3.7. Comparison of three atomic resolution bovine pancreatic PLA_2 structures

The C^α atoms of the present model were superposed on the two atomic resolution structures (Steiner *et al.*, 2001; Sekar *et al.*, 2005) and the most visible differences are limited to only three regions: the surface loop (62–70), the primary calcium-binding loop (30–34) and the C-terminal region (113–123) (Fig. 5). In all other parts, the conformation of the main chain is extremely similar, although some side-chain

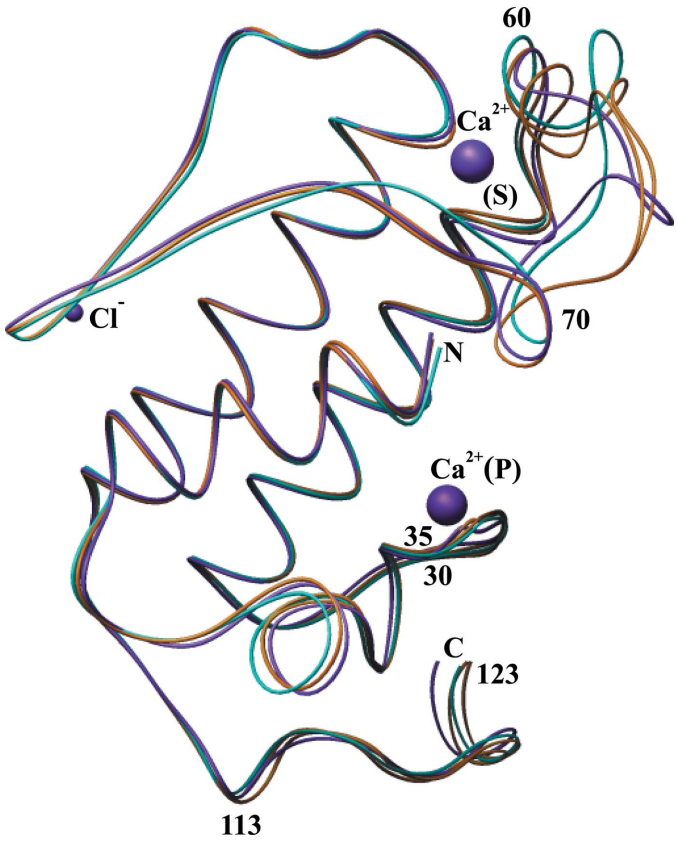

Figure 5
A view of the superposition of the C^{α} atoms of the two atomic resolution structures of PLA_2 and the present model. In the present double-mutant *A* and *B* conformationa are shown in orange, the wild type in cyan and the triple mutant in violet. The positions of the primary calcium ion (P), the second calcium ion (S) and the chloride ion (Cl^-) are also shown. It is clear from the figure that the deviations are more pronounced in the surface loop (region marked 60–70), the calcium-binding loop (30–35) and the C-terminal region (113–123).

conformations vary significantly. The superposition of the backbone atoms of the above three structures gives an r.m.s.d. (root-mean-square deviation) in the range 0.26–1.54 Å. The largest deviations are observed in the surface-loop residues (62–70) and in the C-terminal region (residues 116–123). If the largest deviating residues are omitted from the superposition calculation, the r.m.s.d. range reduces to 0.20–0.70 Å.

3.8. Flexible surface loop

The surface loop (60–70) is always found to be disordered (see, for example, Sekar *et al.*, 1998, 2003; Yu *et al.*, 2000) in most bovine pancreatic PLA_2 structures, with the exception of the orthorhombic form of the wild-type enzyme (Sekar & Sundaralingam, 1999), cryotemperature (Steiner *et al.*, 2001) and second calcium-bound triple mutants (Rajakannan *et al.*, 2002; Sekar *et al.*, 2005). When compared with the ordered surface-loop conformation observed in the orthorhombic form (Sekar & Sundaralingam, 1999) and the anisic acid-bound trigonal form (Sekar *et al.*, 2003), the conformation of the surface loop is different in the second calcium-bound monoclinic form of the triple mutant (Rajakannan *et al.*, 2002; Sekar *et al.*, 2005). In the present structure the surface loop is found to be disordered.

4. Conclusions

A total of five MPD molecules and a chloride ion are located in the present model and these were not identified in the previously reported model refined at 1.9 Å resolution. The second calcium-binding residues Glu92 and Asn72 adopt two different conformations corresponding to second calcium-bound and free forms. Nearly 32% of the atoms adopt alternate conformations.

The facilities at the Supercomputer Education and Research Centre, the Interactive Graphics Molecular Modelling and the Bioinformatics Centre are gratefully acknowledged. One of the authors (DV) thanks the UGC and DBT, India for financial support. DV thanks DST-FIST and UGC-SAP for funding facilities to the Department of Crystallography and Biophysics. The work in MD-T's laboratory is supported by NIH grant GM 41788.

References

Brünger, A. T. (1992). *Nature (London)*, **355**, 472–475.
Deenen van & de Haas, G. H. (1963). *Biochem. Biophys. Acta*, **70**, 538–553.
Dennis, E. A. (1983). *The Enzymes*, 3rd ed., edited by P. D. Boyer, Vol. 16, pp. 307–353. New York: Academic Press.
Dennis, E. A. (1994). *J. Biol. Chem.* **269**, 13057–13060.
Dennis, E. A. (1997). *Trends Biochem. Sci.* **22**, 1–2.
Engh, R. A. & Huber, R. (1991). *Acta Cryst.* A**47**, 392–400.
Harding, M. M. (1999). *Acta Cryst.* D**55**, 1432–1443.
Jain, M. K., Gelb, M. H., Rogers, J. & Berg, O. G. (1995). *Methods Enzymol.* **249**, 567–614.
Jones, T. A. (1985). *Methods Enzymol.* **115**, 157–171.
Moews, P. C. & Kretsinger, R. H. (1975). *J. Mol. Biol.* **91**, 229–232.
Murshudov, G. N., Vagin, A. A. & Dodson, E. J. (1997). *Acta Cryst.* D**53**, 240–255.
Noel, J. P., Bingman, C. A., Deng, T. L., Dupureur, C. M., Hamilton, K. J., Jiang, R. T., Kwak, J. G., Sekharudu, C., Sundaralingam, M. & Tsai, M.-D. (1991). *Biochemistry*, **30**, 11801–11811.
Otwinowski, Z. & Minor, W. (1997). *Methods Enzymol.* **276**, 307–326.
Pieterson, W. A., Vidal, J. C., Volwerk, J. J. & de Haas, G. H. (1974). *Biochemistry*, **13**, 1455–1460.
Rajakannan, V., Yogavel, M., Poi, M.-J., Jeyaprakash, A. A., Jeyakanthan, J., Velmurugan, D., Tsai, M.-D. & Sekar, K. (2002). *J. Mol. Biol.* **324**, 755–762.
Ramachandran, G. N., Ramakrishnan, C. & Sasisekharan, V. (1963). *J. Mol. Biol.* **7**, 95–99.
Ramirez, F. & Jain, M. K. (1991). *Proteins*, **9**, 229–239.
Scott, D. L. & Sigler, P. B. (1994). *Adv. Protein Chem.* **45**, 53–88.
Scott, D. L., White, S. P., Browning, J. L., Rosa, J. J., Gelb, M. H. & Sigler, P. B. (1991). *Science*, **254**, 1007–1010.
Sekar, K., Rajakannan, V., Gayathri, D., Velmurugan, D., Poi, M.-J., Dauter, M., Dauter, Z. & Tsai, M-.D. (2005). *Acta Cryst.* F**61**, 3–7.
Sekar, K., Rajakannan, V., Velmurugan, D., Yamane, T., Thirumurugan, R., Dauter, M. & Dauter, Z. (2004). *Acta Cryst.* D**60**, 1586–1590.
Sekar, K., Sekharudu, C., Tsai, M.-D. & Sundaralingam, M. (1998). *Acta Cryst.* D**54**, 342–346.
Sekar, K. & Sundaralingam, M. (1999). *Acta Cryst.* D**55**, 46–50.
Sekar, K., Vaijayanthi Mala, S., Yogavel, M., Velmurugan, D., Poi, M.-J., Vishwanath, B. S., Gowda, T. V., Jeyaprakash, A. A. & Tsai, M.-D. (2003). *J. Mol. Biol.* **333**, 367–376.
Sheldrick, G. M. (1997). *SHELXL97. A Program for Crystal Structure Refinement.* University of Göttingen, Germany.
Sheldrick, G. M. & Schneider, T. R. (1997). *Methods Enzymol.* **277**, 319–343.
Steiner, R. A., Rozeboom, H. J., de Vries, A., Kalk, K. H., Murshudov, G. N., Wilson, K. S. & Dijkstra, B. W. (2001). *Acta Cryst.* D**57**, 516–526.
Verger, R. (1976). *Annu. Rev. Biophys. Bioeng.* **5**, 77–117.
Yu, B.-Z., Poi, M. J., Ramagopal, U. A., Jain, R., Ramakumar, S., Berg, O. G., Tsai, M.-D., Sekar, K. & Jain, M. K. (2000). *Biochemistry*, **39**, 12312–12323.